Desalination and Water Treatment
www.deswater.com

doi: 10.5004/dwt.2017.21188

84 (2017) 309–323
July

Evaluation of arsenic adsorption capacity of indigenous materials for their suitability as filter media

Sandip Mondal[a,*], Chandan Mahanta[b]

[a]*Department of Earth and Environmental Studies, National Institute of Technology Durgapur, Durgapur 713209, West Bengal, India, Tel. +91-9434789021/+91-343-275-4431; Fax: +91-343-254-7375; email: sandip.mondal@ees.nitdgp.ac.in*
[b]*Department of Civil Engineering, Indian Institute of Technology Guwahati, Guwahati 781039, Assam, India, Tel. +91-361-258-2407; email: chandan@iitg.ernet.in*

Received 13 December 2016; Accepted 7 July 2017

ABSTRACT

Low-cost filter developed with indigenous materials seems to be the only option in rural areas of arsenic contaminated villages in Assam valley. To meet the desired objective, adsorptive properties of some chosen native materials, that is, red soil, sand and naturally oxidized iron scraps (NOISs) are evaluated by conducting a series of batch experiments and surface morphological analysis. The materials have been characterized by field emission scanning electron microscopy and X-ray powder diffraction (XRD) for their morphological study. Batch experiments are performed by changing various parameters including the contact time, pH, temperature, adsorbent dose and initial arsenic [As(III) and As(V)] concentration in the aqueous solutions. Results suggest that the efficiency of the adsorbents in adsorbing both As(III) and As(V) from aqueous solutions sharply declined with increasing pH, particularly for NOIS. The sorption process occurs mainly by intraparticle diffusion followed by film diffusion. The experimental kinetics data can be best described by pseudo-second-order reaction model, while the thermodynamic study showed that the arsenic sorption process is exothermic in nature. The maximum adsorption capacities of red soil, sand and NOIS were found to be 40.26, 19.69 and 166.95 μg g^{-1}, respectively, for the sorption of As(V) from the solution. Such adsorption can be attributed to the amorphous nature of the NOIS, as verified from the XRD patterns. The results indicate that NOIS can be used as promising adsorbent for the removal of arsenic from water.

Keywords: Arsenic; Iron scraps; Sand; Red soil; Adsorption; Indigenous materials; Iron scrap; Batch study; Assam; Groundwater contamination; Kinetic modeling; Thermodynamic study; Diffusion

1. Introduction

Arsenic contamination of groundwater is considered to be one of the biggest human threats being faced by the world in the last three decades [1]. The problem is mainly faced by the people of the Southeast Asia region where four major countries are the worst targets of arsenic contamination [2]. In India, the groundwaters of Ganga–Meghna–Brahmaputra floodplains are highly affected with arsenic contamination due to both anthropogenic and natural causes [3,4]. In order to assess the severity of the newly discovered arsenic contamination in Assam, a study, carried out jointly by The United Nations Children's Fund (UNICEF) and Public Health Engineering Department (PHED) of Assam, found that 18 districts were affected with arsenic contamination [3–6]. Several technologies have already been developed based on oxidation [7,8], adsorption and coprecipitation [9], adsorption [10–13], ion-exchange [14,15], membrane filtration [16,17] and electro-coagulation processes [18] to remove arsenic from drinking water. Many of these processes remove arsenic satisfactorily, both at household and community level. However, water purification cost is a significant issue for rural as well as for semi-urban masses because of their low earnings. Hence, researchers need

---

* Corresponding author.

1944-3994/1944-3986

to develop affordable arsenic removal filtration systems by employing locally available cheap materials. Some low-cost treatment facilities have been already implemented in certain arsenic contaminated areas of Bangladesh, Vietnam and India (West Bengal) since arsenic problems were detected in these places, decades ago [19–21]. Hossain et al. [22] evaluated the efficiency of arsenic removal projects (ARPs) in removing arsenic and iron from raw groundwater. During 2 years of their study, 15 (78%) out of 18 ARPs were no longer in use due to lack of information technology [22]. The literature corroborate that the acceptability and sustainability of the technology depends on the cost associated with the technology (capital and operational cost), complexity system, life of the filter and the effluent quality [22,23]. It has been experienced that successful arsenic removal technologies will not necessarily prosper in the villages of India, unless it fits into the rural circumstances and is well accepted by the consumers [23]. The acceptability of a technology to the rural people enhances when the technology is easy to use and affordable to the users. The main objective of the present study is to evaluate the arsenic adsorption potential of three indigenous materials, that is, naturally oxidized iron scrap (NOIS), sand, and red soil by conducting a series of batch experiments, so that an efficient filtration system can be designed to meet the desired needs of the rural people. The choice of the above substances can be justified by the fact that, sand has been used for long time by people all over the world due to its easy availability and simplicity of usage [24]. In fact, people of Assam are familiar with its usage in water purification as they have used it extensively for the removal of iron from water. Whereas, the usage of red soil and NOIS in this study can be attributed to the fact that iron has the ability to form stable minerals with arsenic. The NOIS can easily be prepared from disposed scrap iron by the users living in the contaminated areas and can be incorporated in the sand filtration unit which are in use in Assam valley for the last few decades. Materials containing iron and iron oxides precipitate out arsenic from the aqueous medium [8,24,25]. The ease of preparation of NOIS from disposed scrap iron and its smooth incorporation in the sand filtration units, used by the people of the Assam valley, may be stated as the other important reason for us to use it as an adsorbent in this work.

2. Materials and methods

2.1. Preparation and characteristics of adsorbents

Naturally available river sand, red soil and NOIS have been used in the present study. Sand was collected from a river in the vicinity and red soil was collected from a local hill. NOIS was collected from a local mechanical workshop where the iron scraps were produced regularly after various cutting and filing operations. These scraps were disposed into an open chamber where these were naturally oxidized in the open atmosphere. The collected sand and NOIS were washed with distilled water to ensure that there were no impurities left on their external surface. The washed materials were dried in the oven at 105°C ± 2°C for 24 h and then allowed to cool at room temperature. Thereafter the particles were sieved to get the desired particle size. The maximum particle size of NOIS was restricted to 2 mm. In case of sand, 425 µm to 2 mm sized particles were used to make it silt free. The collected red soil was allowed to dry at room temperature. The dried red soil particles were crushed using rubber hammer and passed through 425 µm sieve. After which the red soil particles were collected and stored for adsorption study.

The major oxides compositions of the sand, red soil and NOIS were determined by X-ray fluorescence spectrometry analysis (Model: AXIOS, PANalytical, Location: Philips). The obtained results (Table 1) indicate the presence of iron oxide in NOIS and red soil that may facilitate the adsorption of arsenic from aqueous solution. The Fourier-Transform Infrared Spectroscopy (FTIR) spectra of the NOIS were analyzed in KBr pellets using Perkin-Elmer 281 IR spectrophotometer. The properties of NOIS, sand and red soil have been summarized in Table 2.

The degree of lateritization of the red soil was estimated from the silica–sesquioxide (S–S) ratio ($SiO_2/(Fe_2O_3 + Al_2O_3)$). The soil type can be characterized from the obtained value of the degree of lateritization using following values:

- < 1.33: laterite soil
- 1.33–2: lateritic soil
- > 2: non-lateritic, tropical soil

Degree of lateritization for red soil is 1.77, indicating that the soil is lateritic soil.

The surface morphological study of the sand and NOIS was carried out by using scanning electron microscope (Model: LEO, 1430 VP, Carl Zeiss, Location: Germany) as shown in Fig. 1. The surface of NOIS was characterized by field emission scanning electron microscopy (FESEM; Sigma, Zeiss) images. From the images of Fig. 1, it can be seen that the sand and red soil particles are irregular in

Table 1
Major oxide compositions of the adsorbents (all the values in wt%)

Adsorbent	Red soil	Sand	NOIS
SiO_2	57.61	70.08	23.14
Al_2O_3	24.31	14.46	9.53
Fe_2O_3 (total)	8.23	4.40	52.29
MnO	0.16	0.15	0.48
MgO	1.10	0.58	0.14
CaO	0.58	1.22	0.07
Na_2O	2.25	3.06	2.18
K_2O	4.09	3.37	0.28
TiO_2	1.36	0.42	0.14
P_2O_5	0.20	0.12	0.53

Table 2
Properties of the adsorbents (sand, NOIS and red soil)

Properties	NOIS	Red soil	Sand
Particle size range (mm)	<2	<0.425	0.425–2
Mean particle size diameter (µm)	801	20	653
Density (g cm^{-3})	5.03	2.54	2.65
Bulk density (g cm^{-3})	2.74	1.31	1.51

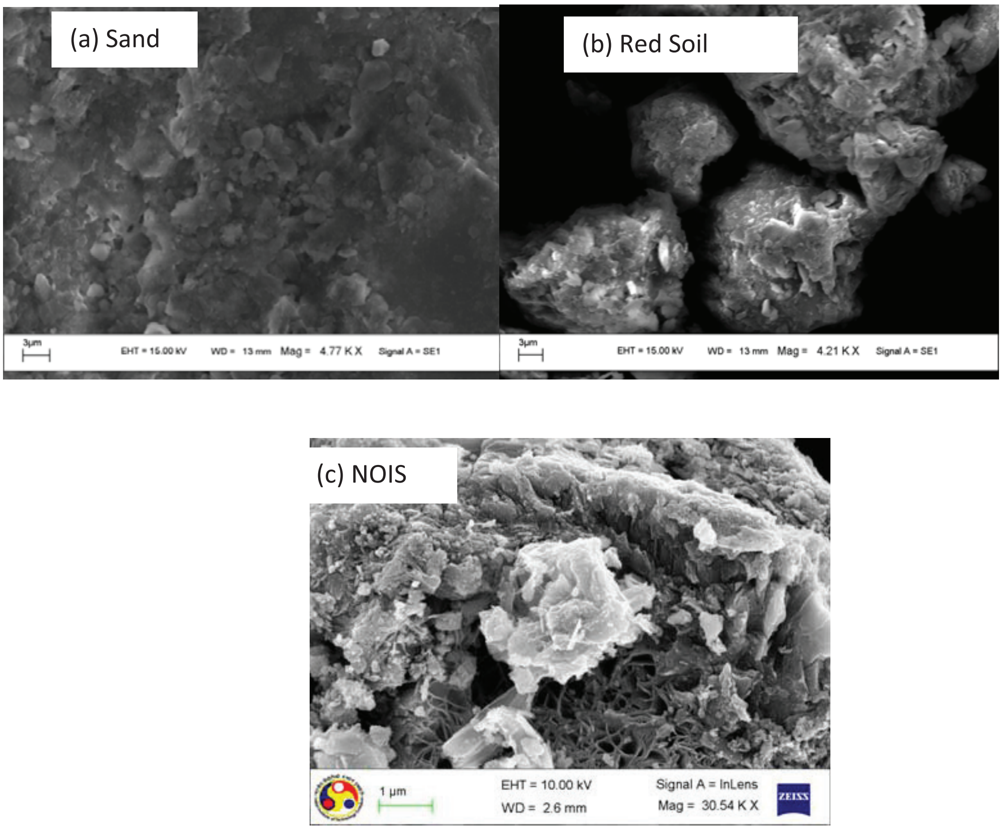

Fig. 1. SEM images of (a) sand, (b) red soil and (c) NOIS.

shape with sharp edges whereas NOIS particles have irregular shape with high porosity.

The major and minor mineralogical composition of the adsorbents were identified using X-ray powder diffraction (XRD) system (Model: XRD 3003TT, SEIFFRT, Rich Seifert & Co., Ahrensburg, Germany) with Cu Kα radiation (λ = 1.54 Å), a Cu filter on secondary optics, 45 kV voltage and 20 mA current. The XRD profiles of the samples were measured in the range of 10°–95° with the step size of 0.05°/s.

The obtained characteristic strong peaks (Fig. 2(a)) in the case of sand were related to quartz (JCPD file no. 05-490). Absence of other prominent peaks in the XRD pattern confirms that quartz is the major component of sand. The XRD pattern (Fig. 2(b)) indicates that red soil contained quartz, maghemite, goethite and kaolinite. The XRD pattern of NOIS indicates the absence of sharp peaks, thus confirming the amorphous nature of the particles (Fig. 2(c)). Kulal et al. [26] synthesized amorphous phase of Fe_2O_3 and used them for supercapacitor application. They stated that the amorphous nature of the material allowed easy diffusion of ions through the bulk of the material. Hence, it may be possible that the amorphous phase allows better removal by facilitating the adsorption process through bulk diffusion of ions [26–29].

The FTIR spectra for NOIS before and after adsorption of arsenic (Fig. S1), shows peaks at 3,434 and 3,436 cm^{-1} (nearby 3,400 cm^{-1}), which can be assigned to the –OH stretching vibrations of the water molecules coordinated to the trivalent cations (Fe^{3+} or Al^{3+}) [30] and the corresponding peaks at 1,637 and 1,632 cm^{-1} due to –OH bending [31]. Peak at 597 cm^{-1} confirmed that NOIS contain α-Fe_2O_3 whereas peak at 562 cm^{-1} indicated the presence of γ-Fe_2O_3 in the NOIS after adsorption of arsenic [32]. Again peak at 880 cm^{-1} represents $AsO(OH)_2^-$ species [33] confirming the presence of arsenic adsorption by the NOIS.

2.2. Reagents and analytical methods

All the chemicals used were of analytical grade and used without further purification. HPLC grade ultrapure water was obtained from Chemiton water purification system (CHEMITON SL, Spain, Model no. QRP-380 BC) and was used for preparation of all the reagents and aqueous solutions. 1,000 mg L^{-1} arsenic stock solutions were prepared using required amounts of arsenic trioxide (As_2O_3; Merck, India, AR grade) for As(III) solutions and sodium arsenate ($Na_2HAsO_4.7H_2O$; Merck, India, AR grade) for the As(V) solutions. The stock solutions were preserved with 1% trace metal grade nitric acid. Required standard and experimental solutions were prepared from the stock solutions by serial dilution for arsenic standardization and experimental purposes. Aqueous As(III) and As(V) samples were analyzed for total arsenic by atomic absorption spectrometry (Spectra AA Varian, Australia, Model no. 55B) with vapor generation accessory (VGA-77) in the form of AsH_3 at a wavelength of 193.7 nm. All the samples were pre-reduced with 5% KI–ascorbic acid solution (KI; Merck, India, AR grade and l-ascorbic acid; Merck, India, AR grade) under highly acidic conditions using HCl (Suprapur grade, Merck, Germany).

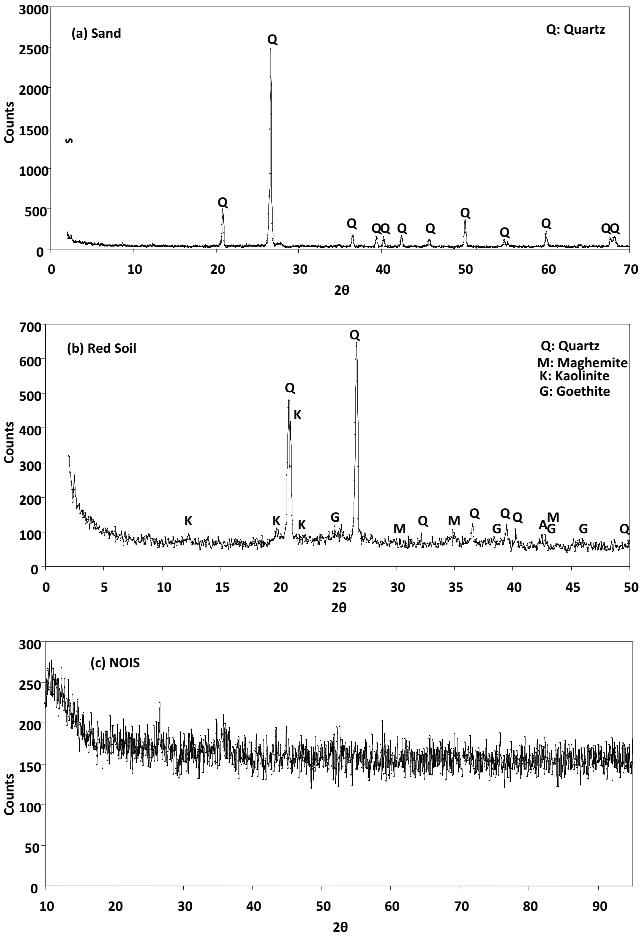

Fig. 2. XRD patterns of (a) sand, (b) red soil and (c) NOIS.

2.3. Experimental methods

All batch experiments were carried out for the selected adsorbents (sand, red soil and NOIS) using synthetic As(III) and As(V) spiked solution, which are prepared by diluting respective stock solutions by distilled water. Before conducting the experiments, all the glassware were soaked in dilute HNO_3 for 24 h and then washed with tap water and finally with distilled water. The batch sorption studies were performed at 25°C ± 1°C in an incubator shaker (Daihan Labtech Co. Ltd., Korea, Model no. LSI-1005R) at an agitation speed of 200 rpm. 100 mL As(III) or As(V) samples (having concentration 200 μg L^{-1}) with fixed amount of adsorbents (red soil: 1 g, NOIS: 0.5 g and sand: 2 g) were taken into 250 mL conical flasks and covered with aluminium foil. The samples were placed in the incubator shaker for fixed span of time. For each experiment, separate conical flasks were used. In the all cases, at the end of the experiments, the supernatant of the samples were filtered with Whatman-42 filter paper and were preserved with 1 mL 1:1 HCl for arsenic assessment. The kinetic studies were carried out using fixed amount of adsorbent in appropriate amount of arsenic spiked solution at constant strength and temperature varying the contact time of the samples. The isotherm study was conducted by varying the adsorbent dose in the samples at equilibrium time. To determine the effect of pH on arsenic sorption onto the adsorbents, the experiments were performed at different pH in the range of 0.94–12.37. Desired pH of the arsenic spiked solution was adjusted using 1 N NaOH and 1 N HCl. The thermodynamics study was conducted at different temperatures of 10°C, 25°C, 40°C and 55°C for an initial concentration of 200 μg g^{-1} at constant adsorbent dose (sand: 2 g, NOIS: 0.5 g and red soil: 1 g). The effect of initial arsenic concentration was checked by varying the initial arsenic strength (100, 200, 300 and 500 μg L^{-1}) for both As(III) and As(V) species at equilibrium time.

2.4. Adsorption capacity

The amount of arsenic species adsorbed at time *t*, which is known as adsorption capacity, q_t (μg g^{-1}) is calculated from the mass balance equation as below [34]:

$$q_t = \frac{(C_0 - C_t)V}{m} \tag{1}$$

where C_0 is the initial concentration (μg L^{-1}), C_t is the concentration of the arsenic spiked solution at time *t* (μg L^{-1}), *V* is the volume of sample (L) and *m* is the mass of adsorbent (g). The amount of arsenic species adsorbed at the equilibrium, q_e, is calculated from Eq. (1), when *t* is equal to the equilibrium contact time, $C_t = C_e$, $q_e = q_t$.

3. Results and discussion

3.1. Effect of pH on arsenic sorption

Arsenic sorption from aqueous medium onto adsorbent is governed by the pH of the medium. Arsenic sorption onto all the adsorbents was same in the acidic media whereas under alkaline conditions, the arsenic adsorption capacity of NOIS and red soil rapidly decreased with increasing of pH as shown in Fig. 3(a). The adsorption capacity of sand remained almost unaffected with the increase of pH throughout the studied range. Generally, it is found that As(III) remains in the solution in the neutral state as H_3AsO_3 from the pH range of 3–8.5 [35]. A positive surface charge on the surface of the sorbent acts as the driving force for the adsorption process in this pH range [33–35]. Fig. 3(b) indicates that As(V) sorption on the adsorbents was influenced by the pH of the solution. Similar results can also be noticed for As(V) sorption onto laterite iron [25,33,35–39], ferric hydroxides and titanium dioxide nanoparticles [40,41]. Neutral arsenate (H_3AsO_4) exists in the aqueous medium only below pH 2 under oxidizing conditions; whereas, its presence has been observed in the solution in the form of $HAsO_4^-$ and $HAsO_4^{2-}$ even at normal condition [36].

3.2. Effect of contact time

From the experiment, it was found that uptake capacity of sorbate is faster in the initial stage of sorption process, thereafter, it decreases as the solute concentration reaches equilibrium [33,42–45]. In Figs. 4(a) and (b), similar observation has been noted for the both As(III) and As(V) sorption

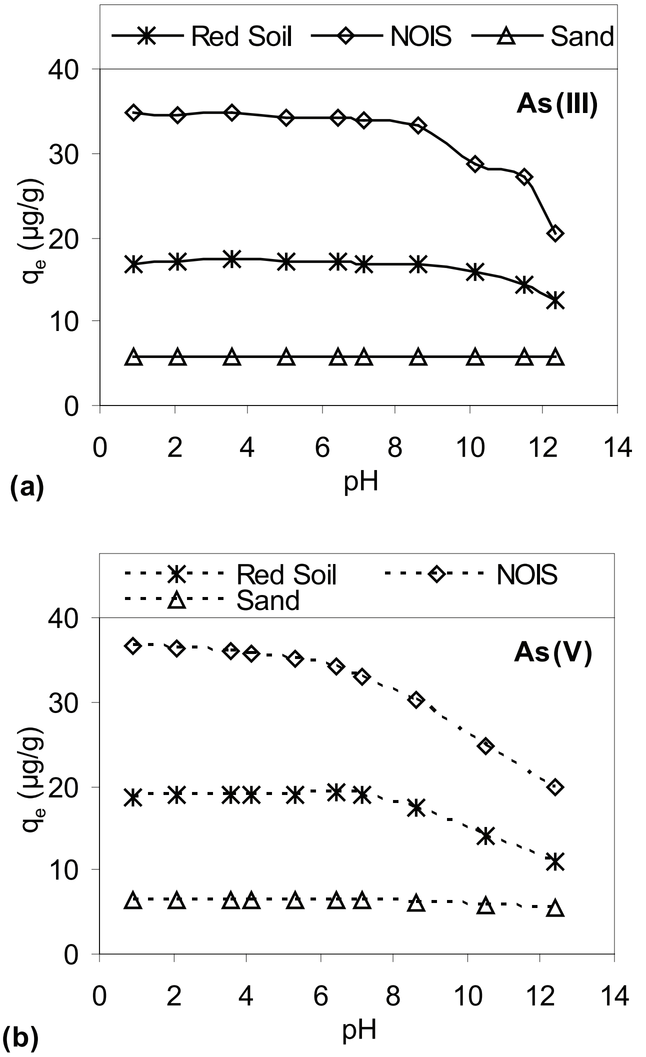

Fig. 3. Effect of pH on arsenic sorption onto red soil, NOIS and sand.

onto the adsorbents. It may be possible that initially a large number of vacant sites were available for the sorbate; but as time progresses, remaining vacant sites were difficult to access for the sorbate due to repulsive force between the solute molecules present in the solid and bulk phase [46]. Result shows that maximum quantities of arsenic were adsorbed by all the adsorbents within 120 min of the adsorption process. The initial uptake rate of NOIS is high in comparison with the other adsorbents. To achieve 80% removal efficiency, NOIS took only 15 min for As(V) and 30 min for As(III) species.

3.3. Kinetic modeling

Adsorption is a time dependent process and it is very important to find out the equilibrium contact time, rate of adsorption and sorption mechanism for design and evaluation of the adsorption mechanism for removal of arsenic species from water [47,48]. The essential stages in the adsorption processes are:

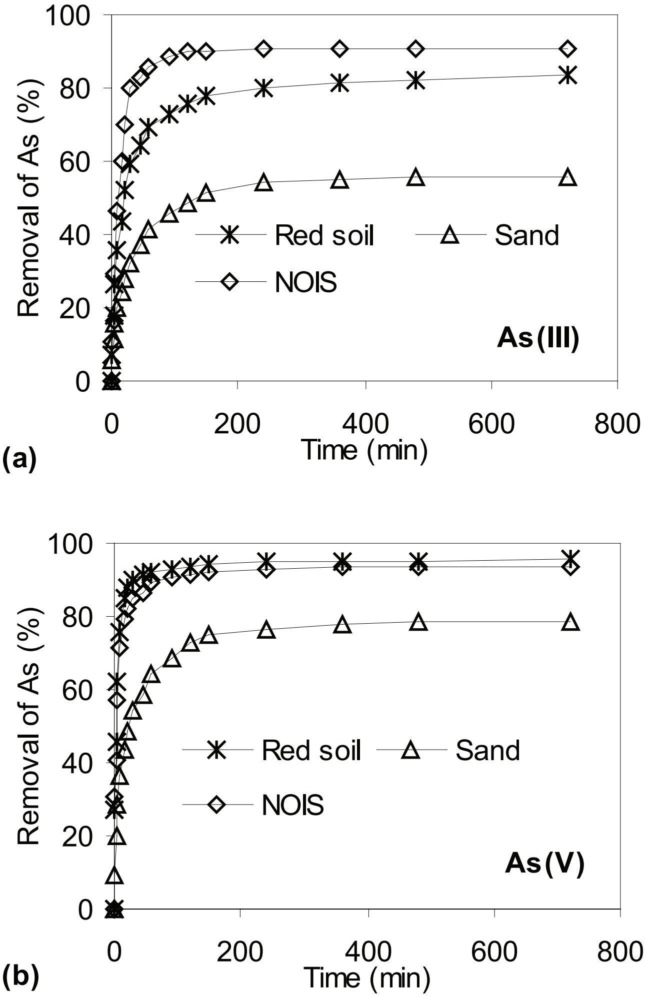

Fig. 4. Dynamics of arsenic adsorption onto red soil, sand and NOIS [matrix: initial As(III) or As(V) concentration = 200 µg L^{-1}, volume of sample = 100 mL, agitation speed = 200 rpm, temperature = 25°C ± 1°C and pH = 7].

- Film diffusion
- Pore diffusion
- Intraparticle diffusion

In order to investigate the arsenic adsorption rate and sorption mechanism onto the adsorbents (red soil, sand and NOIS), the pseudo-second-order reaction model, the intraparticle diffusion model, the film diffusion model, the liquid film mass transfer model and the Richenberg model were analyzed [49].

3.3.1. Pseudo-second-order reaction model

The pseudo-second-order reaction model or second-order rate expression of Lagergren is based on the adsorption capacity of adsorbent. It may be expressed in the form [46]:

$$\frac{dq}{dt} = k_{s2}(q_e - q_t)^2 \tag{2}$$

where k_{s2} is the rate constant of pseudo-second-order adsorption (g µg^{-1} min^{-1}). Integration of Eq. (2) for boundary condition $t = 0$ to $t = t$ and $q_t = 0$ to $q_t = q_e$ gives:

$$\frac{t}{q_t} = \frac{1}{k_{s2}q_e^{\ 2}} + \frac{t}{q_e} \tag{3}$$

The validity of the model can be checked by linear plot of t/q_t vs. t. q_e and k_{s2} can be obtained from the slope and intercept of the linear plot. In Fig. S2, straight-line plots of t/q_t vs. t represented pseudo-second-order reaction model that was obtained from the experimental data. The evaluated parameters of the pseudo-second-order reaction model are summarized in Table 3. High correlation coefficient (R^2) values and low standard error (SE) values confirm that the kinetics of the arsenic sorption by the selected materials followed pseudo-second-order reaction model. Maji et al. [35] got similar results for arsenic sorption onto the laterite soil [49].

3.3.2. Intraparticle diffusion model

Intraparticle diffusion model or parabolic diffusion model developed by Weber and Morris (1963) is also frequently used to describe the adsorption kinetics. The model can be express as [8,50]:

$$q_t = k_i t^{1/2} + C_i \tag{4}$$

where k_i is the intraparticle diffusion rate constant (µg g^{-1} min$^{-1/2}$) and C_i (µg g^{-1}) the constant that gives idea about the thickness of the boundary layer (Cabal et al. [51]). k_i and C_i can be calculated from the slope and intercept of linear plot of q_t vs. $t^{1/2}$.

Table 3
Comparison of pseudo-second-order reaction model parameters for the arsenic adsorption onto different adsorbents

Adsorbent	As species	q_e (µg g^{-1})	K_{s2} (g µg^{-1} min^{-1})	R^2	SE
Red soil	As(III)	16.946	0.0046	0.9999	0.317
	As(V)	19.214	0.0206	1.0000	0.270
Sand	As(III)	5.720	0.0098	0.9994	0.246
	As(V)	7.992	0.0107	0.9999	0.282
NOIS	As(III)	36.887	0.0042	0.9998	2.019
	As(V)	37.613	0.0087	1.0000	0.849

Plots of q_t vs. t of the kinetic data of the selected adsorbents are representing the intraparticle diffusion model (Fig. S3). The correlated parameters are summarized in Table 4. In Figs. S3(a) and (b), multiple lines are assuring that the adsorption process consists of several sorption mechanisms. Cheung et al. [52] found similar observation for the sorption of an acid dye onto chitosan. The first portion of the graph, started from the origin indicating external diffusion or film diffusion. Steepness of the line is the evidence of rapid sorption. The second portion gradually increased with the square root of time, indicating that the intraparticle diffusion is the rate-limiting step in this stage. Last portion of the curve is almost parallel to the x-axis, confirming the retardation of intraparticle diffusion and existence of low concentration of sorbate in the solute [52,53].

3.3.3. Liquid film mass transfer model

Boyd, Adamson and Myers derived an equation assuming that the adsorption process is controlled by film diffusion and the concentration gradient is negligible. The equation can be written as [8,54–56]:

$$\ln(1 - F) = K_1 t \tag{5}$$

where F is the fraction of the solute and k_1 is the adsorption rate constant (min^{-1}). The constant value can be obtained from the plot of $\ln(1 - F)$ vs. t. The initial adsorption rate constant can be evaluated from the given expression as the initial rapid adsorption of solute is controlled by the film diffusion [47].

The values obtained from the plots of $\ln(1 - F)$ vs. t (Fig. S4) have been shown in Table 5. Good R^2 values are supporting the applicability of this model and is the evidence of the film diffusion is the controlling step at initial stage. Remaining non-linear portion of the plot is confirming that film diffusion is not the rate-limiting step; some other diffusion processes are also involved in the sorption process. In Table 5, it can be seen that the film diffusion rate constants (K_1) are greater for As(V) sorption from aqueous medium than As(III). The K_1 values for NOIS and red soil are higher than sand, indicating different degrees of affinities of the sorbent for arsenic species. It may be possible that red soil and NOIS contain iron oxides, causing arsenic adsorption and enhancing the uptake capacity.

Initial adsorption kinetic coefficient can be determined by Adam–Bohart–Thomas equation. It can be expressed as [57]:

$$\gamma = K_{\text{sorp}} q_m = -\frac{V}{C_0 m}\left(\frac{dC_t}{dt}\right)_{t\to 0} \tag{6}$$

Table 4
Parameters of the intraparticle diffusion rate constant

Adsorbent	As species	K_{i1}	$R_{i1}^{\ 2}$	C_{i2}	K_{i2}	$R_{i2}^{\ 2}$	C_{i3}	K_{i3}	$R_{i3}^{\ 2}$
Red soil	As(III)	2.25	0.992	10.03	0.46	0.963	15.20	0.057	0.988
	As(V)	4.81	0.959	6.50	0.26	0.965	18.46	0.029	0.851
Sand	As(III)	0.62	0.990	2.10	0.25	0.982	5.37	0.007	0.725
	As(V)	1.08	0.975	4.13	0.28	0.971	7.37	0.019	0.859
NOIS	As(III)	5.95	0.975	28.07	0.75	0.969	35.98	0.017	0.841
	As(V)	9.71	0.974	28.67	0.91	0.963	36.01	0.061	0.827

Table 5
Adsorption kinetics and mass transfer coefficients of arsenic sorption onto studied adsorbent

Adsorbent	Arsenic species	K_1 (min^{-1})	R^2	γ (L μg^{-1} m^{-1}) × 10^{-3}	k_fA_s (m^3 s^{-1}) × 10^{-4}	R^2
Red soil	As(III)	0.0517	0.9451	7.11	3.97	0.9377
	As(V)	0.1391	0.9315	17.91	12.10	0.8948
Sand	As(III)	0.0168	0.9715	2.20	1.87	0.8096
	As(V)	0.0230	0.8700	3.95	3.81	0.8497
NOIS	As(III)	0.0715	0.9978	12.79	6.15	0.9961
	As(V)	0.1216	0.8932	31.19	10.19	0.8425

where K_{sorp} (L μg^{-1} min^{-1}) is the adsorption kinetic constant and γ (L μg^{-1} m^{-1}) is the initial adsorption kinetic coefficient. The values of the kinetic coefficient were determined using the initial slope of the plots between solute concentration and time and the values of the initial kinetic coefficients are depicted in Table 5. The γ values are approximately two times higher for As(V) than As(III). For the As(V) sorption, maximum value 17.91 × 10^{-3} L μg^{-1} m^{-1} is found for NOIS whereas minimum value 3.95 × 10^{-3} L μg^{-1} m^{-1} is obtained for the sand.

Mathews and Weber proposed the initial estimation of liquid film mass transfer model and that can be expressed as [47,58]:

$$V\frac{dC}{dt} = k_f A_s (C - C_s) \tag{7}$$

where V is the volume of arsenic spiked solution (L), k_f is the liquid film mass transfer coefficient (m^2 s^{-1}), C_s is the liquid-phase concentration at external sorbent surface (μg L^{-1}) and A_s is the surface area of adsorbent. Integrating Eq. (7) at $t \to 0$, $C_s \to 0$ gives [59]:

$$-\ln\left(\frac{C}{C_0}\right) = k_f \frac{A_s}{V} t \tag{8}$$

The value of k_fA_s, which is known as global external transport coefficient (m^3 s^{-1}), can be calculated from the slope of linear plot of –ln (C/C$_0$) vs. time (t). The values of k_fA_s for the studied adsorbents are determined instead of k_f to standardize the material adsorption properties. The obtained results are presented in Table 5.

3.3.4. Richenberg model

The Richenberg model was developed to check the sorption process is based on film diffusion or intraparticle diffusion mechanism and that can be written in the following form [54,60]:

$$\frac{q_t}{q_e} = \left(1 - \frac{6}{\pi^2}\right)\exp(Bt) \tag{9}$$

Bt can be calculated for each value of q_t as:

$$Bt = -0.4977\ln\left(1 - \frac{q_t}{q_e}\right) \tag{10}$$

The intraparticle diffusion will be the sole rate-controlling step, if linear plot of Bt vs. t passes through the origin [61]. The non-linear plots of the kinetic data are the evidence of intraparticle diffusion and it is not a rate-limiting step (not shown here).

3.4. Thermodynamics evaluation of arsenic adsorption

To observe the effect of temperature on arsenic sorption onto the red soil, sand and NOIS thermodynamics study was conducted. The thermodynamic equilibrium constant (K_c) can be evaluated from the following expression [62]:

$$K_c = \frac{C_a}{C_e} \tag{11}$$

where C_e (μg L^{-1}) is the equilibrium arsenic concentration in solution and C_a (μg L^{-1}) is the concentration of arsenic adsorbed at equilibrium. The thermodynamic parameters can be evaluated from the following equations [61–64]:

$$\Delta G^\circ = -RT\ln K_C \tag{12}$$

$$\Delta G^\circ = \Delta H^\circ - T\Delta S^\circ \tag{13}$$

where ΔG°, ΔH° and ΔS° are the Gibb's free energy of arsenic sorption (kJ mol^{-1}), enthalpy (kJ mol^{-1}) and entropy (J mol^{-1} K^{-1}) change of adsorption, respectively [61]. T is the adsorption temperature (K) and R is the universal gas constant (8.314 J mol^{-1} K^{-1}). The K_c may be expressed as a function of temperature using the following expression [61]:

$$\ln K_c = -\frac{\Delta H^\circ}{RT} + \frac{\Delta S^\circ}{R} \tag{14}$$

The values of ΔH° and ΔS° can be evaluated from the slop and intercept of the plot of K_c vs. $1/T$ (Van't Hoff plot). The Van't Hoff plots (lnK_c vs. $1/T$) for arsenic [As(III) and As(V)] sorption onto red soil, sand and NOIS are shown in Fig. S5. The evaluated thermodynamic parameters using Eqs. (12) and (13) are summarized in Table 6. From the Van't Hoff plots, negative values of change in enthalpy (ΔH°) and entropy (ΔS°) are obtained. From Table 6, it can be seen that Gibb's free energy of arsenic sorption (ΔG°) values are negative except for As(III) sorption using sand at 328 K. Negative ΔG° values confirm that the adsorption process is feasible and spontaneous in nature [62]. Increasing of ΔG° values with temperature indicates that the adsorption process is

Table 6
Evaluated thermodynamic parameters of both As(III) and As(V) sorption onto red soil, sand and NOIS

Adsorbent	Temperature (K)	As(III)			As(V)		
		$\Delta G°$ (kJ mol^{-1})	$\Delta H°$ (kJ mol^{-1})	$\Delta S°$ (J mol^{-1} K^{-1})	$\Delta G°$ (kJ mol^{-1})	$\Delta H°$ (kJ mol^{-1})	$\Delta S°$ (J mol^{-1} K^{-1})
Red soil	283	–4.95	–16.65	–41.35	–8.70	–33.43	–87.37
	298	–4.33			–7.39		
	313	–3.71			–6.08		
	328	–3.09			–4.77		
Sand	283	–1.04	–10.09	–31.98	–3.78	–16.09	–43.49
	298	–0.56			–3.13		
	313	–0.08			–2.48		
	328	0.40			–1.82		
NOIS	283	–6.15	–18.39	–43.23	–7.53	–26.99	–68.75
	298	–5.51			–6.50		
	313	–4.86			–5.47		
	328	–4.21			–4.44		

not favorable at higher temperature [65]. The negative values of change in enthalpy ($\Delta H°$) of both As(III) and As(V) sorption confirm that the adsorption process is exothermic in nature. Further negative values of entropy change ($\Delta S°$) in both cases indicate that the degree of freedom of solute molecules decreases as the adsorbate adsorbed onto the surface of adsorbent [40,61].

3.5. Equilibrium study

Equilibrium study is important to describe the adsorption system of adsorbents and to optimize the design adsorption mechanism of adsorbate. Several isotherm models have been used to describe the equilibrium characteristics of adsorption [46,66]. In this study, Langmuir [67], Freundlich [68,69], Redlich–Peterson [70,71] and Temkin [64,72] methods were used to interpret the obtained equilibrium values.

3.5.1. Langmuir isotherm

Langmuir developed the isotherm assuming that fixed number of equal energetically one molecular thick site are available for adsorption and there is no interaction between adsorbed molecules of neighbor sites [72–74]. The isotherm can be represented as:

$$\frac{q_e}{q_m} = \frac{bC_e}{1 + bC_e} \tag{15}$$

where C_e is the solute concentration of adsorbate at equilibrium (μg L^{-1}), q_e is the amount of adsorbate adsorbed at equilibrium (μg g^{-1}), q_m is the maximum adsorption capacity of adsorbent, b is the Langmuir constant which is directly related to Henry constant ($K' = bq_m$). Eq. (15) can be rewritten as [47,50]:

$$\frac{C_e}{q_e} = \frac{1}{bq_m} + \frac{C_e}{q_m} \tag{16}$$

Table 7
Langmuir isotherm parameters of various adsorbents

Adsorbent	As species	q_m (μg g^{-1})	b (L μg^{-1})	R^2	R_L	Remarks
Red soil	As(III)	21.86	0.0136	0.9906	0.27	Favorable
	As(V)	46.44	0.0124	0.9932	0.29	Favorable
Sand	As(III)	17.16	0.0066	0.9991	0.43	Favorable
	As(V)	23.81	0.0138	0.9937	0.27	Favorable
NOIS	As(III)	155.60	0.0064	0.9670	0.44	Favorable
	As(V)	245.10	0.0056	0.9289	0.47	Favorable

The above model is known as type 1 Langmuir isotherm. Plot of C_e/q_e vs. C_e gives good fit over wide concentration ranges and represents qualitative type 1 isotherm form.

Weber and Chakravorti [58] expressed the favorable nature and the essential characteristics of adsorption isotherm in terms of a dimensionless separation factor that is defined by [61]:

$$R_L = \frac{1}{1 + bC_0} \tag{17}$$

where b is the Langmuir constant and C_0 is the initial adsorbate concentration (μg L^{-1}).The value of R_L indicates the type of isotherm which can be expressed as irreversible adsorption ($R_L = 0$), favorable adsorption ($0 < R_L < 1$), linear ($R_L = 0$) and unfavorable adsorption ($R_L > 1$) [47].

Langmuir isotherm constants for arsenic sorption onto different adsorbents are determined by linear regression method by plotting C_e/q_e vs. C_e and the results are depicted in Table 7. The result shows that the dimensionless R_L values (0.27–0.47) lie within favorable limit for each adsorbent. The R^2 values of red soil and sand are above 0.99 which suggest that the adsorption isotherm follows the Langmuir model. R^2 values of NOIS are found to be 0.96 for As(III) and 0.92

for As(V), respectively. Moderate values of R^2 indicate that the Langmuir isotherm may not be a good model for arsenic sorption onto NOIS.

3.5.2. Freundlich isotherm

Freundlich developed an empirical equation applicable to adsorption onto heterogeneous surface composed of different classes of adsorption sites with adsorption in each class following the Langmuir isotherm. The isotherm is defined as follows [12,68,69]:

$$q_e = K_F C_e^{1/n} \tag{18}$$

where K_F is constant related to adsorption capacity of the adsorbent (µg$^{1-(1/n)}$ L$^{1/n}$ g^{-1}) and n is the Freundlich empirical constant depending on the heterogenic properties of adsorbent [47,66]. The Freundlich equation can be liberalized as follows:

$$\ln q_e = \ln K_F + (1/n)\ln C_e \tag{19}$$

where K_F and n values can be evaluated from the linear plot of $\ln q_e$ vs. $\ln C_e$, if the sorption process obeys Freundlich model. The maximum adsorption capacity (q_m) of the sorbent can be evaluated from Halsey equation using constant initial concentration C_0 and variable weight of the adsorbent. The equation is defined as [47,75].

$$K_F = \frac{q_m}{C_0^{1/n}} \tag{20}$$

Freundlich isotherms parameters for the experimental data of the studied adsorbent are presented in Table 8. Higher correlation coefficient values indicate that the Freundlich model delineates the sorption isotherm better than the Langmuir model. The values of n varying from 1.16 to 1.77 indicate the favorable adsorption of arsenic on the sorbent. The maximum adsorption capacity determined by Freundlich model is found to be almost the same or lower than the Langmuir model.

3.5.3. The Redlich–Peterson isotherm

The Redlich–Peterson (R–P) isotherm is combined form of Langmuir and Freundlich isotherm. It approaches the Freundlich isotherm at high concentrations and is in accordance with the low concentration limit of the Langmuir isotherm. The R–P isotherm is expressed as [66,71,76]:

$$q_e = \frac{K_R C_e}{1 + \alpha_R C_e^{\beta}} \tag{21}$$

where K_R (L g^{-1}) and α_R (L µg^{-1}) are the isotherm constants and β is the constant with the value lies between 0 and 1. For β = 1, the equation will perform as Langmuir and for β = 0, it will reduce to Henry equation.

The linear form of Eq. (21) can be written as:

$$\ln\left(K_R \frac{C_e}{q_e} - 1\right) = \ln\alpha_R + \beta \ln C_e \tag{22}$$

where K_R, α_R and β can be determined using non-linear regression method.

The R–P equation was solved by minimizing root mean square errors (RMSEs) and maximizing the correlation coefficient (R^2) between predicted data for q_e and the experimental equilibrium data, using the solver add-in function in MS excel spreadsheet. The R–P isotherm constants for arsenic sorption are summarized in Table 9. Low RMSE value and high correlation coefficient (R^2) confirming the best fit of experimental data in the R–P model.

3.5.4. Temkin isotherm

The Temkin isotherm is based on the following assumptions [66,73]:

- The heat of adsorption of all the molecules in the layer decreases linearly with coverage due to adsorbent–adsorbate interactions.
- The sorption is characterized by a uniform distribution of the binding energies, up to some maximum binding energy.

The equation of the Temkin isotherm can be written as follows [47]:

$$\frac{q_e}{q_m} = \frac{RT}{\Delta Q}\ln(K_0 C_e) \tag{23}$$

Table 8
Freundlich parameters for arsenic removal by various adsorbents

Adsorbent	As species	K_F (µg$^{1-(1/n)}$ L$^{1/n}$ g^{-1})	n	q_m (µg g^{-1})	R^2
Red soil	As(III)	0.899	1.77	17.82	0.9911
	As(V)	1.156	1.49	40.26	0.9866
Sand	As(III)	0.345	1.56	10.35	0.9928
	As(V)	0.941	1.74	19.69	0.9924
NOIS	As(III)	1.352	1.21	109.73	0.9981
	As(V)	1.700	1.16	166.95	0.9994

Table 9
Comparison of R–P isotherm parameters for arsenic sorption by the adsorbents

Adsorbent	As species	α_R (L µg^{-1})	β	K_R (L g^{-1})	R^2	RMSE
Red soil	As(III)	0.0639	0.7742	0.3998	0.9971	0.0363
	As(V)	0.0227	0.9028	0.6194	0.9902	0.0935
Sand	As(III)	0.0100	0.8172	0.1072	0.9771	0.0701
	As(V)	0.0758	0.7483	0.4529	0.9997	0.0126
NOIS	As(III)	0.0815	0.5438	1.2000	0.9932	0.0499
	As(V)	0.1990	0.3690	1.8640	0.9883	0.0460

The equation can be expressed as:

$$\frac{q_e}{q_m} = \frac{RT}{\Delta Q}\ln K_0 + \frac{RT}{\Delta Q}\ln C_e \tag{24}$$

where R is the universal gas constant (8.314 J mol^{-1} K^{-1}), T is the absolute temperature (K), ΔQ is the energy transmission during sorption of the sorbate (kJ mol^{-1}) and K_0 is the Temkin constant (L µg^{-1}). Values of ΔQ and K_0 can be calculated from the linear plot of q_e/q_m vs. lnC_e.

To plot the Temkin equation, the maximum adsorption capacity (q_m) is derived from Freundlich equation. The Temkin isotherm plots and the parameters are depicted in Table 10. Positive adsorption energy (ΔQ) indicates that the adsorption reaction is exothermic. Moderate R^2 values of the studied adsorbents indicate that the Temkin model cannot represent the equilibrium data satisfactory.

From all the results of the equilibrium study (Tables 7–10), based on the correlation coefficient, it may be concluded that Freundlich model is the best-fit model for the adsorption of arsenic. However, Langmuir and R–P models are also applicable for describing the equilibrium data. The isotherm models can be arranged in order of excellent fit of the equilibrium data as: Freundlich > Redlich–Peterson > Langmuir > Temkin. The experimental data confirm that NOIS can remove arsenic to a greater extent. Based on the adsorption capacity, the materials can be arranged in the following order: NOIS > red soil > sand. A comparative analysis has been drawn here to show the efficiency of the used materials. A comparative analysis of the arsenic removal by different adsorbent is presented in Table 11.

Table 10
Temkin isotherm parameters of red soil, sand and NOIS

Adsorbents	As species	K_0 (µg L^{-1})	ΔQ (kJ mol^{-1})	R^2
Red soil	As(III)	0.1380	9.33	0.9850
	As(V)	0.1718	11.44	0.9685
Sand	As(III)	0.0628	6.76	0.9958
	As(V)	0.1439	9.59	0.9851
NOIS	As(III)	0.2055	15.08	0.8786
	As(V)	0.2587	18.26	0.8467

3.6. Effect of initial arsenic concentration

The effects of initial As(III) and As(V) concentration on the removal capacity of NOIS, red soil and sand are presented in Fig. 5. Results indicate that as the initial arsenic concentration increased the removal efficiency of the adsorbents decreased for both As(III) and As(V). In case of red soil and sand, there was appreciable decrease in removal percentage with increase in concentration of arsenic sample. This may be because of the fact that for the lower adsorbate concentration, sufficient amounts of free sites are available which results maximum removal of the adsorbate. Whereas for higher adsorbate concentration, limited sites of the sorbents remain to be occupied by the adsorbate molecules. The excess amounts of adsorbate remain in the solution. Both As(III) and As(V) removal efficiencies for NOIS were slightly decreased whereas the initial arsenic concentration was increased to a greater extent. This is because of the fact that the adsorption capacity of the NOIS is higher; hence, many free sites are available for arsenic adsorption. Although the arsenic concentration in the bulk solution was increased significantly, vacant sites were still available for adsorption.

4. Conclusions

In the present study, the adsorption characteristics of the low-cost adsorbent, that is, red soil, sand and NOIS for the removal of arsenic from aqueous solution has been investigated in batch mode. XRD patterns confirmed that the NOIS particles were amorphous in nature, which may facilitate better arsenic removal. All of the adsorbents were efficient

Table 11
Comparative analysis of arsenic sorption capacity of various adsorbents

S. No.	Material taken	Initial As concentration	As sorption capacity (mg g^{-1})	Reference
1	Manganese ore	–	0.53	[8]
2	Portland cement	0.2 mg L^{-1}	3.98	[8]
3	Modified calcined bauxite	0.5 mg L^{-1}	1.37	[8]
4	Iron oxide-coated sand	100 µg L^{-1}	0.136	[77]
5	Red mud	33.37 µmol L^{-1}	0.663	[78]
6	Biomass of *Rhizopus oryzae*	100 mg L^{-1}	0.047	[79]
7	Magnesia loaded-fly ash cenospheres	50 mg L^{-1}	–	[80]
8	Haematite	–	31.3	[81]
9	Magnetite	–	25.6	[81]
10	Goethite	–	12.5	[81]
11	Iron-coated pottery granules	150 mg L^{-1}	1.17	[82]
12	FBBS	5 mg L^{-1}	59.7	[83]
13	Sand	250 µg L^{-1}	0.00572	This work
14	Red soil	250 µg L^{-1}	0.01695	This work
15	NOIS	250 µg L^{-1}	0.0367	This work

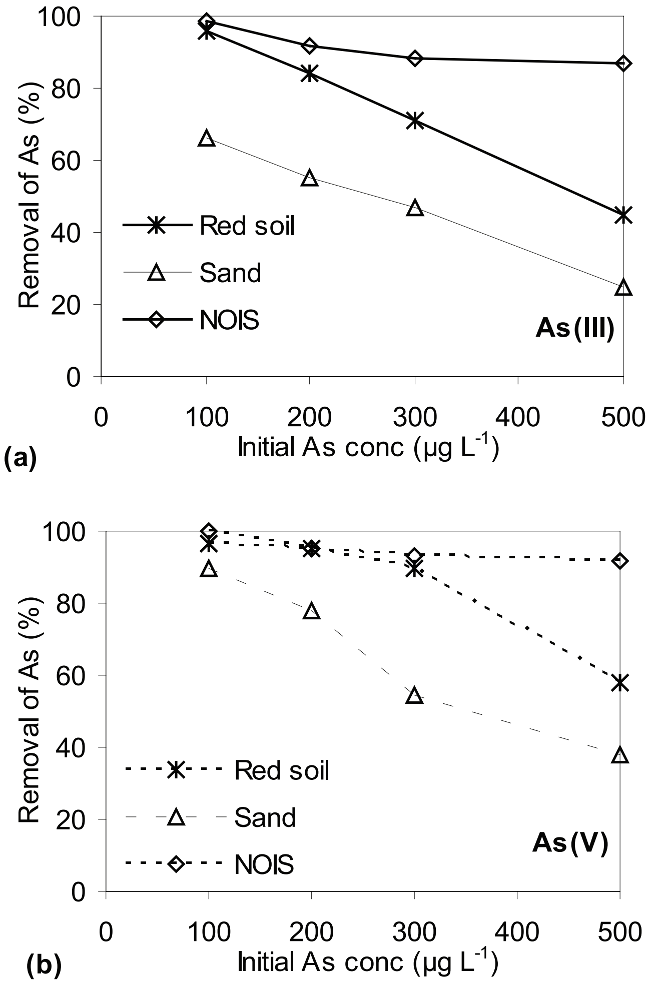

Fig. 5. Effect of initial arsenic concentration for the adsorption of (a) As(III) and (b) As(V) onto the surface of NOIS, sand and red soil [matrix: initial arsenic concentration = 200 µg L^{-1}, volume of the solution = 100 mL, temperature = 25°C ± 1°C and pH = 6.96].

in adsorbing arsenic under acidic medium, whereas under alkaline condition, the removal efficiency of arsenic was rapidly decreased with increasing the pH of the solution. Adsorption kinetics of arsenic sorption onto the adsorbents followed Lagergren pseudo-second-order reaction model. The arsenic sorption process consisted of two phases. Initial rapid sorption was controlled by film diffusion whereas comparatively slower second phase of the adsorption process was controlled by intraparticle diffusion. The thermodynamic study showed that the adsorption processes of all adsorbents were exothermic in nature. The experimental equilibrium data obtained were applied to several isotherm models. Results revealed that the Freundlich isotherm was the best-fit model. From the interpretation of the equilibrium data, the isotherm models can be arranged in the order of excellent fit as Freundlich > Redlich–Peterson > Langmuir > Temkin. The maximum adsorption capacity (q_m) was found to be highest for NOIS [109.73 µg g^{-1} for As(III) and 245.10 µg g^{-1} for As(V)]. Initial arsenic concentration of the solution affected the arsenic removal efficiency for the studied adsorbents. Adsorbent efficiency decreased with increasing the arsenic concentration in the solution. The batch studies ensured that the NOIS can be used as promising adsorbent for arsenic remediation in developing indigenous treatment technologies.

Acknowledgment

The authors wish to express their gratitude to the Department of Civil Engineering, IIT Guwahati for providing the support for the current work.

References

[1] M.M. Rahman, R. Naidu, P. Bhattacharya, Arsenic contamination in groundwater in the Southeast Asia region, Environ. Geochem. Health, 31 (2009) 9–21.

[2] A. Mukherjee, M.K. Sengupta, M.A. Hossain, S. Ahamed, B. Das, B. Nayak, D. Lodh, M.M. Rahman, D. Chakraborti, Arsenic contamination in groundwater: a global perspective with emphasis on the Asian scenario, J. Health Popul. Nutr., 24 (2006) 142–163.

[3] C. Mahanta, R. Choudhury, S. Basu, R. Hemani, A. Dutta, P.P. Barua, P.J. Borah, M. Bhattacharya, K. Bhattacharya, W. Alam, L. Saikia, A. Mukherjee, P. Bhattacharya, Preliminary Assessment of Arsenic Distribution in Brahmaputra River Basin of India Based on Examination of 56,180 Public Groundwater Wells, Safe and Sustainable Use of Arsenic-Contaminated Aquifers in the Gangetic Plain: A Multidisciplinary Approach, Springer International Publishing, Cham, 2015, pp. 57–64.

[4] B.A. Shah, Arsenic Contamination in Groundwater in the Middle Gangetic Plain, India: Its Relations to Fluvial Geomorphology and Quaternary Stratigraphy, A.L. Ramanathan, S. Johnston, A. Mukherjee, B. Nath, Eds., Safe and Sustainable Use of Arsenic-Contaminated Aquifers in the Gangetic Plain: A Multidisciplinary Approach, Springer International Publishing, Cham, 2015, pp. 33–53.

[5] S. Mishra, S. Dwivedi, A. Kumar, J. Mattusch, R. Tripathi, Current status of ground water arsenic contamination in India and recent advancements in removal techniques from drinking water, Int. J. Plant Environ., 2 (2016) 1–2.

[6] D. Saha, S. Sahu, A decade of investigations on groundwater arsenic contamination in Middle Ganga Plain, India, Environ. Geochem. Health, 38 (2016) 315–337.

[7] P. Mondal, C. Majumder, B. Mohanty, Treatment of arsenic contaminated water in a laboratory scale up-flow bio-column reactor, J. Hazard. Mater., 153 (2008) 136–145.

[8] D. Mohan, C.U. Pittman, Arsenic removal from water/wastewater using adsorbents—a critical review, J. Hazard. Mater., 142 (2007) 1–53.

[9] X. Meng, G.P. Korfiatis, C. Christodoulatos, S. Bang, Treatment of arsenic in Bangladesh well water using a household co-precipitation and filtration system, Water Res., 35 (2001) 2805–2810.

[10] D. Qu, J. Wang, D. Hou, Z. Luan, B. Fan, C. Zhao, Experimental study of arsenic removal by direct contact membrane distillation, J. Hazard. Mater., 163 (2009) 874–879.

[11] D.M. Sahabi, M. Takeda, I. Suzuki, J.-i. Koizumi, Adsorption and abiotic oxidation of arsenic by aged biofilter media: equilibrium and kinetics, J. Hazard. Mater., 168 (2009) 1310–1318.

[12] S. Chen, Q. Yue, B. Gao, X. Xu, Equilibrium and kinetic adsorption study of the adsorptive removal of Cr (VI) using modified wheat residue, J. Colloid Interface Sci., 349 (2010) 256–264.

[13] M.R.I. Chowdhury, C.N. Mulligan, Biosorption of arsenic from contaminated water by anaerobic biomass, J. Hazard. Mater., 190 (2011) 486–492.

[14] J. Kim, M.M. Benjamin, Modeling a novel ion exchange process for arsenic and nitrate removal, Water Res., 38 (2004) 2053–2062.

[15] P. Chutia, S. Kato, T. Kojima, S. Satokawa, Arsenic adsorption from aqueous solution on synthetic zeolites, J. Hazard. Mater., 162 (2009) 440–447.

[16] J. Ćurko, I. Mijatović, M. Matošić, H.K. Jakopović, M.U. Bošnjak, As(V) removal from drinking water by coagulation and filtration through immersed membrane, Desalination, 279 (2011) 404–408.

[17] L. Melita, M. Popescu, Removal of Cr (VI) from industrial water effluents and surface waters using activated composite membranes, J. Membr. Sci., 312 (2008) 157–162.

[18] X. Zhao, B. Zhang, H. Liu, J. Qu, Removal of arsenite by simultaneous electro-oxidation and electro-coagulation process, J. Hazard. Mater., 184 (2010) 472–476.

[19] O.E.A. Salam, N.A. Reiad, M.M. ElShafei, A study of the removal characteristics of heavy metals from wastewater by low-cost adsorbents, J. Adv. Res., 2 (2011) 297–303.

[20] H.-T. Fan, T. Sun, H.-B. Xu, Y.-J. Yang, Q. Tang, Y. Sun, Removal of arsenic(V) from aqueous solutions using 3-[2-(2-aminoethylamino)ethylamino]propyl-trimethoxysilane functionalized silica gel adsorbent, Desalination, 278 (2011) 238–243.

[21] V. Gupta, Application of low-cost adsorbents for dye removal – a review, J. Environ. Manage., 90 (2009) 2313–2342.

[22] M.A. Hossain, M.K. Sengupta, S. Ahamed, M.M. Rahman, D. Mondal, D. Lodh, B. Das, B. Nayak, B.K. Roy, A. Mukherjee, Ineffectiveness and poor reliability of arsenic removal plants in West Bengal, India, Environ. Sci. Technol., 39 (2005) 4300–4306.

[23] Y. Wang, D.C.W. Tsang, Effects of solution chemistry on arsenic(V) removal by low-cost adsorbents, J. Environ. Sci., 25 (2013) 2291–2298.

[24] B. Das, P. Hazarika, G. Saikia, H. Kalita, D.C. Goswami, H.B. Das, S.N. Dube, R.K. Dutta, Removal of iron from groundwater by ash: a systematic study of a traditional method, J. Hazard. Mater., 141 (2007) 834–841.

[25] P.B. Bhakat, A.K. Gupta, S. Ayoob, S. Kundu, Investigations on arsenic(V) removal by modified calcined bauxite, Colloids Surf., A, 281 (2006) 237–245.

[26] P. Kulal, D. Dubal, C. Lokhande, V. Fulari, Chemical synthesis of Fe_2O_3 thin films for supercapacitor application, J. Alloys Compd., 509 (2011) 2567–2571.

[27] R. Balasubramaniam, A.R. Kumar, P. Dillmann, Characterization of rust on ancient Indian iron, Curr. Sci., 85 (2003) 1546–1555.

[28] K. Asami, M. Kikuchi, In-depth distribution of rusts on a plain carbon steel and weathering steels exposed to coastal–industrial atmosphere for 17 years, Corros. Sci., 45 (2003) 2671–2688.

[29] T. Gujar, V. Shinde, C. Lokhande, W.-Y. Kim, K.-D. Jung, O.-S. Joo, Spray deposited amorphous RuO_2 for an effective use in electrochemical supercapacitor, Electrochem. Commun., 9 (2007) 504–510.

[30] K. Liu, Q. Chen, H. Hu, Z. Yin, Characterization and leaching behaviour of lizardite in Yuanjiang laterite ore, Appl. Clay Sci., 47 (2010) 311–316.

[31] G. Anbalagan, A. Prabakaran, S. Gunasekaran, Spectroscopic characterization of Indian standard sand, J. Appl. Spectrosc., 77 (2010) 86–94.

[32] B. Suresh, T. Sowmya, S. Sankaranarayanan, Synthesis of iron oxide from metallurgical wastes, J. Min. Metall. Sect. B, 45 (2009) 127–130.

[33] F. Partey, D. Norman, S. Ndur, R. Nartey, Arsenic sorption onto laterite iron concretions: temperature effect, J. Colloid Interface Sci., 321 (2008) 493–500.

[34] Y. Tian, M. Wu, R. Liu, D. Wang, X. Lin, W. Liu, L. Ma, Y. Li, Y. Huang, Modified native cellulose fibers—a novel efficient adsorbent for both fluoride and arsenic, J. Hazard. Mater., 185 (2011) 93–100.

[35] S.K. Maji, A. Pal, T. Pal, A. Adak, Sorption kinetics of arsenic on laterite soil in aqueous medium, J. Environ. Sci. Health, Part A, 42 (2007) 989–996.

[36] F.Y. Alshaebi, W.Z.W. Yaacob, A.R. Samsudin, Removal of arsenic from contaminated water by selected geological natural materials, Aust. J. Basic Appl. Sci., 4 (2010) 4413–4422.

[37] R.R. Frost, R.A. Griffin, Effect of pH on adsorption of arsenic and selenium from landfill leachate by clay minerals, Soil Sci. Soc. Am. J., 41 (1977) 53–57.

[38] M. Debasish, M. Debaraj, P.K. Ho, A laboratory scale study on arsenic(V) removal from aqueous medium using calcined bauxite ore, J. Environ. Sci., 20 (2008) 683–689.

[39] L. Sailo, C. Mahanta, Natural attenuation processes of arsenic in the groundwater of the Brahmaputra floodplain of Assam, India, Environ. Sci. Processes Impacts, 18 (2016) 115–125.

[40] E. Valencia-Trejo, M. Villicaña-Méndez, R. Alfaro-Cuevas-Villanueva, M. Garnica-Romo, R. Cortés-Martínez, Effect of temperature on the removal of arsenate from aqueous solutions by titanium dioxide nanoparticles, J. Appl. Sci. Environ. Sanit., 5 (2010) 171–84.

[41] X. Meng, S. Bang, G.P. Korfiatis, Effects of silicate, sulfate, and carbonate on arsenic removal by ferric chloride, Water Res., 34 (2000) 1255–1261.

[42] R. Chen, C. Zhi, H. Yang, Y. Bando, Z. Zhang, N. Sugiur, D. Golberg, Arsenic (V) adsorption on Fe_3O_4 nanoparticle-coated boron nitride nanotubes, J. Colloid Interface Sci., 359 (2011) 261–268.

[43] Y.H. Chen, Y.D. Chen, Kinetic study of Cu(II) adsorption on nanosized $BaTiO_3$ and $SrTiO_3$ photocatalysts, J. Hazard. Mater., 185 (2011) 168–173.

[44] M. Islam, P.C. Mishra, R. Patel, Arsenate removal from aqueous solution by cellulose-carbonated hydroxyapatite nanocomposites, J. Hazard. Mater., 189 (2011) 755–763.

[45] P.M. Choksi, V.Y. Joshi, Adsorption kinetic study for the removal of nickel (II) and aluminum (III) from an aqueous solution by natural adsorbents, Desalination, 208 (2007) 216–231.

[46] I.D. Mall, V.C. Srivastava, N.K. Agarwal, Removal of Orange-G and Methyl Violet dyes by adsorption onto bagasse fly ash—kinetic study and equilibrium isotherm analyses, Dyes Pigm., 69 (2006) 210–223.

[47] O. Hamdaoui, Batch study of liquid-phase adsorption of methylene blue using cedar sawdust and crushed brick, J. Hazard. Mater., 135 (2006) 264–273.

[48] T.S. Singh, K. Pant, Equilibrium, kinetics and thermodynamic studies for adsorption of As(III) on activated alumina, Sep. Purif. Technol., 36 (2004) 139–147.

[49] A. Violante, M. Pigna, Competitive sorption of arsenate and phosphate on different clay minerals and soils, Soil Sci. Soc. Am. J., 66 (2002) 1788–1796.

[50] W.J. Weber, J.C. Morris, Kinetics of adsorption on carbon from solution, J. Sanit. Eng. Div., 89 (1963) 31–60.

[51] B. Cabal, C.O. Ania, J.B. Parra, J.J. Pis, Kinetics of naphthalene adsorption on an activated carbon: comparison between aqueous and organic media, Chemosphere, 76 (2009) 433–438.

[52] W. Cheung, Y. Szeto, G. McKay, Intraparticle diffusion processes during acid dye adsorption onto chitosan, Bioresour. Technol., 98 (2007) 2897–2904.

[53] Y.S. Ho, J.C. Ng, G. McKay, Kinetics of pollutant sorption by biosorbents, Sep. Purif. Methods, 29 (2000) 189–232.

[54] D. Reichenberg, Properties of ion-exchange resins in relation to their structure. III. Kinetics of exchange, J. Am. Chem. Soc., 75 (1953) 589–597.

[55] F. Helfferich, M.S. Plesset, Ion exchange kinetics. A nonlinear diffusion problem, J. Chem. Phys., 28 (1958) 418–424.

[56] D. Mohan, K.P. Singh, V.K. Singh, Removal of hexavalent chromium from aqueous solution using low-cost activated carbons derived from agricultural waste materials and activated carbon fabric cloth, Ind. Eng. Chem. Res., 44 (2005) 1027–1042.

[57] R. Djeribi, O. Hamdaoui, Sorption of copper(II) from aqueous solutions by cedar sawdust and crushed brick, Desalination, 225 (2008) 95–112.

[58] A.P. Mathews, W.J. Weber Jr., Physical, chemical wastewater treatment, AIChE Symp. Ser, 166 (1976) 91–98.

[59] K.K. Choy, D.C. Ko, C.W. Cheung, J.F. Porter, G. McKay, Film and intraparticle mass transfer during the adsorption of metal ions onto bone char, J. Colloid Interface Sci., 271 (2004) 284–295.

[60] V.K. Gupta, M. Gupta, S. Sharma, Process development for the removal of lead and chromium from aqueous solutions using red mud—an aluminium industry waste, Water Res., 35 (2001) 1125–1134.

[61] D. Ranjan, M. Talat, S. Hasan, Biosorption of arsenic from aqueous solution using agricultural residue ‘rice polish’, J. Hazard. Mater., 166 (2009) 1050–1059.

[62] P.K. Pandey, S. Choubey, Y. Verma, M. Pandey, K. Chandrashekhar, Biosorptive removal of arsenic from drinking water, Bioresour. Technol., 100 (2009) 634–637.

[63] P.A. Kumar, S. Chakraborty, Fixed-bed column study for hexavalent chromium removal and recovery by short-chain polyaniline synthesized on jute fiber, J. Hazard. Mater., 162 (2009) 1086–1098.

[64] A. Maiti, J.K. Basu, S. De, Experimental and kinetic modeling of As(V) and As(III) adsorption on treated laterite using synthetic and contaminated groundwater: effects of phosphate, silicate and carbonate ions, Chem. Eng. J., 191 (2012) 1–12.

[65] B. Sarkar, N. Venkateswralu, R.N. Rao, C. Bhattacharjee, V. Kale, Treatment of pesticide contaminated surface water for production of potable water by a coagulation-adsorption-nanofiltration approach, Desalination, 212 (2007) 129–140.

[66] C.A. Başar, Applicability of the various adsorption models of three dyes adsorption onto activated carbon prepared waste apricot, J. Hazard. Mater., 135 (2006) 232–241.

[67] V. Gupta, V. Saini, N. Jain, Adsorption of As(III) from aqueous solutions by iron oxide-coated sand, J. Colloid Interface Sci., 288 (2005) 55–60.

[68] S. Kundu, A. Gupta, Arsenic adsorption onto iron oxide-coated cement (IOCC): regression analysis of equilibrium data with several isotherm models and their optimization, Chem. Eng. J., 122 (2006) 93–106.

[69] W.J. Weber Jr., T.C. Voice, A. Jodellah, Adsorption of humic substances: the effects of heterogeneity and system characteristics, J. Am. Water Works Assoc., 75 (1983) 612–619.

[70] A. Örnek, M. Özacar, İ.A. Şengil, Adsorption of lead onto formaldehyde or sulphuric acid treated acorn waste: equilibrium and kinetic studies, Biochem. Eng. J., 37 (2007) 192–200.

[71] O. Redlich, D.L. Peterson, A useful adsorption isotherm, J. Phys. Chem., 63 (1959) 1024–1024.

[72] B. Manna, U.C. Ghosh, Adsorption of arsenic from aqueous solution on synthetic hydrous stannic oxide, J. Hazard. Mater., 144 (2007) 522–531.

[73] M. Temkin, The kinetics of some industrial heterogeneous catalytic reactions, Adv. Catal., 28 (1979) 173–291.

[74] D.M. Ruthven, Principles of Adsorption and Adsorption Processes, John Wiley & Sons (United States), 1984, pp. 48–52.

[75] G.D. Halsey, The role of surface heterogeneity in adsorption, Adv. Catal., 4 (1952) 259–269.

[76] P.S. Kumar, S. Ramalingam, C. Senthamarai, M. Niranjanaa, P. Vijayalakshmi, S. Sivanesan, Adsorption of dye from aqueous solution by cashew nut shell: studies on equilibrium isotherm, kinetics and thermodynamics of interactions, Desalination, 261 (2010) 52–60.

[77] O.S. Thirunavukkarasu, T. Viraraghavan, K.S. Subramanian, O. Chaalal, M.R. Islam, Arsenic removal in drinking water—impacts and novel removal technologies, Energy Sources, 27 (2005) 209–219.

[78] H.S. Altundogan, S. Altundogan, F. Tumen, M. Bildik, Arsenic adsorption from aqueous solutions by activated red mud, Waste Manage., 22 (2002) 357–363.

[79] D. Pokhrel, T. Viraraghavan, Arsenic removal from aqueous solution by iron oxide-coated biomass: common ion effects and thermodynamic analysis, Sep. Sci. Technol., 43 (2008) 3545–3562.

[80] Q. Li, X. Xu, H. Cui, J. Pang, Z. Wei, Z. Sun, J. Zhai, Comparison of two adsorbents for the removal of pentavalent arsenic from aqueous solutions, J. Environ. Manage., 98 (2012) 98–106.

[81] M. Chiban, M. Zerbet, G. Carja, F. Sinan, Application of low-cost adsorbents for arsenic removal: a review, J. Environ. Chem. Ecotoxicol., 4 (2012) 91–102.

[82] S.A. Baig, T. Sheng, Y. Hu, J. Xu, X. Xu, Arsenic removal from natural water using low cost granulated adsorbents: a review, CLEAN Soil Air Water, 43 (2015) 13–26.

[83] K. Wu, R. Liu, T. Li, H. Liu, J. Peng, J. Qu, Removal of arsenic(III) from aqueous solution using a low-cost by-product in Fe-removal plants—Fe-based backwashing sludge, Chem. Eng. J., 226 (2013) 393–401.

Supplementary information

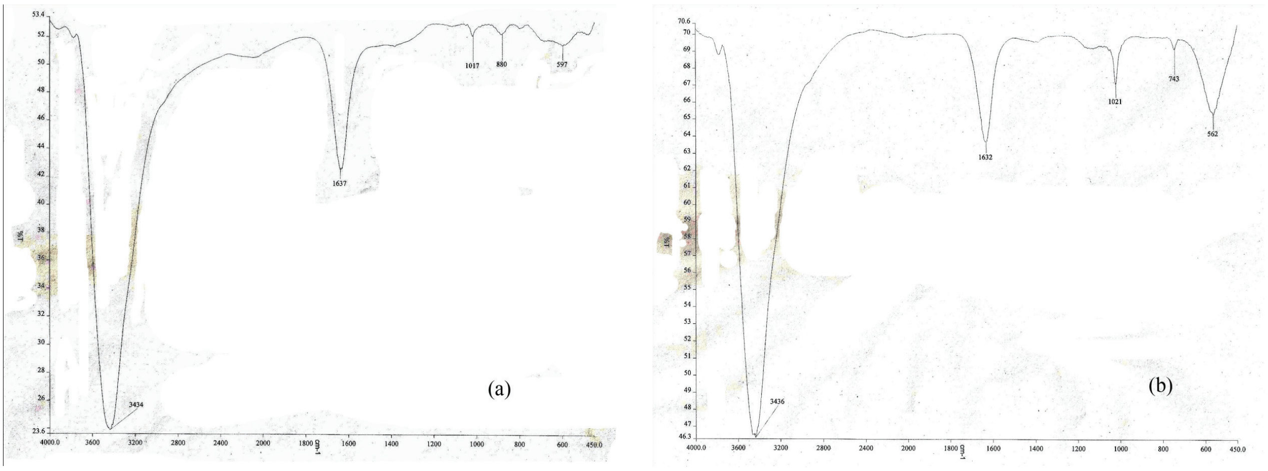

Fig. S1. FTIR spectra of NOIS (a) before and (b) after adsorption of arsenic.

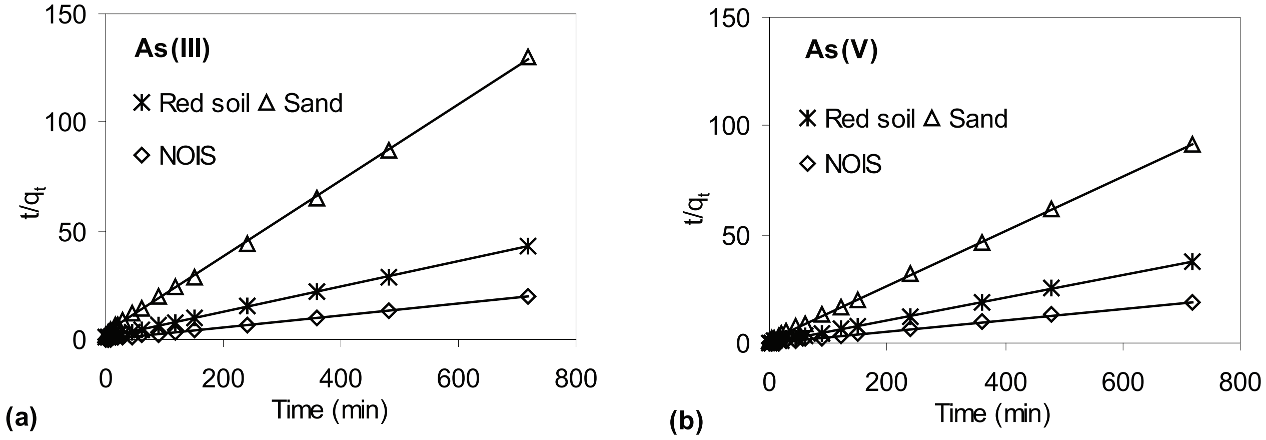

Fig. S2. Test of pseudo second order reaction model for arsenic [As(III) and As(V)] adsorption onto different material.

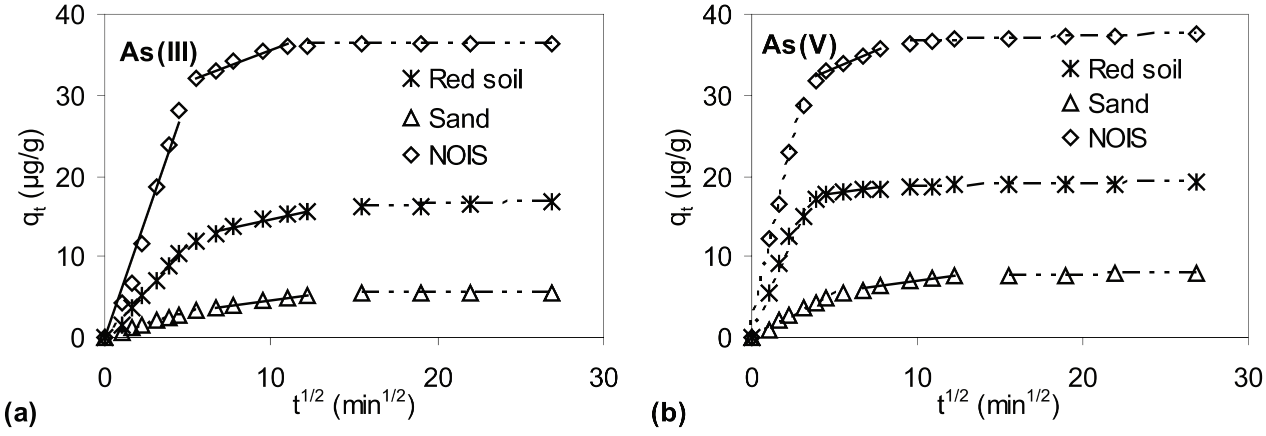

Fig. S3. Plots of intraparticle diffusion for arsenic [As(III) and As(V)] sorption onto different adsorbent.

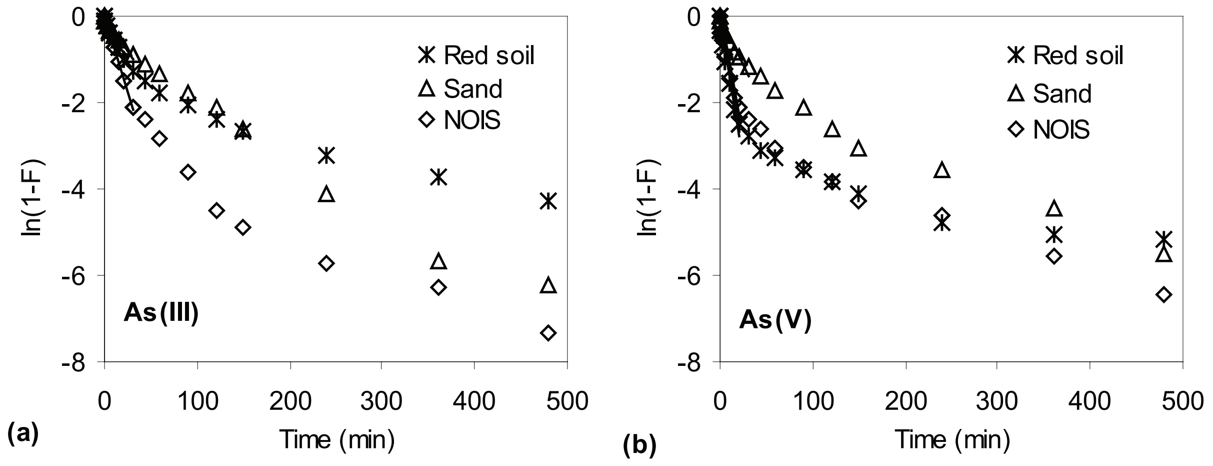

Fig. S4. Plots of ln(1 – *F*) vs. *t* for arsenic adsorption onto different adsorbent.

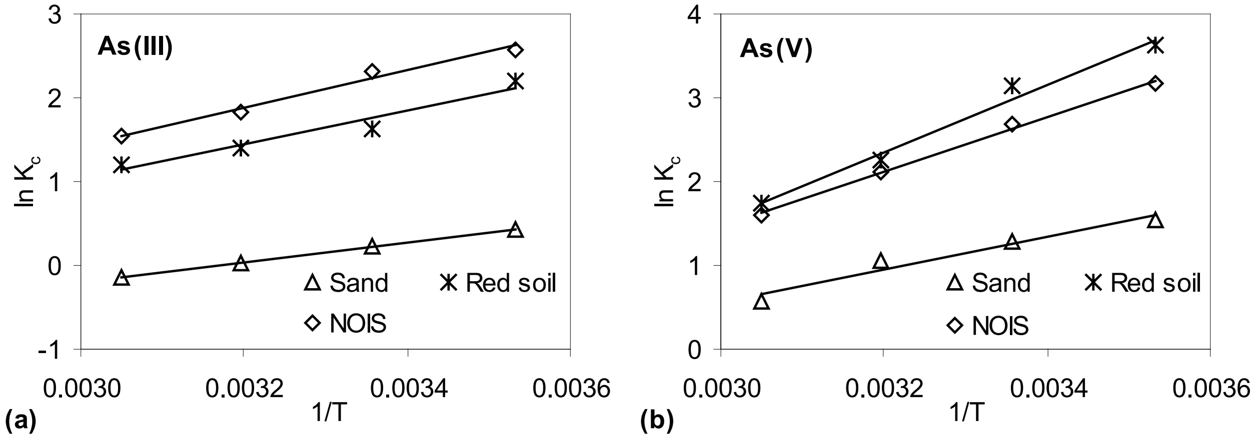

Fig. S5. Thermodynamic study of arsenic sorption onto NOIS, sand and red soil.